



# Dosimetry of indoor alpha flux belonging to seasonal radon, thoron and their EECs

Anjali Kaushal · Manish Joshi · Amit Sarin · Navjeet Sharma

Received: 25 March 2021 / Accepted: 23 December 2021 / Published online: 24 January 2022  
© The Author(s), under exclusive licence to Springer Nature Switzerland AG 2022

**Abstract** Radon ( $^{222}\text{Rn}$ ) and thoron ( $^{220}\text{Rn}$ ) are ubiquitous radioactive noble gases present in the earth's crust. The source term for these gases includes soil and building materials as well. The radiological impact of radon/thoron gases and their decay products on human life is a matter of concern and has been given due attention in research and policy. The present study aims to measure and quantify residential radon/thoron gas and the decay product's concentration and to discuss the associated interpretations for Ludhiana district of Punjab, India. Passive measurement techniques employing a single-entry pinhole dosimeter for gases and direct progeny sensors for the decay product's concentration have been used in this work. The obtained data from these measurements have been analysed using appropriate statistical techniques. The variations have been

linked with the changes in the ventilation conditions, building material, room type and altitude. A higher concentration of radon and thoron gas was observed in the winter season for the study region. It was estimated that the contribution of radon and thoron decay products towards the annual average inhalation dose is 75% and 25%, respectively.

**Keywords** Radon · Thoron · Progeny · Pinhole dosimeter · Inhalation dose · Seasonal dependence

## Introduction

Exposure of human beings to the ionizing radiations present in the natural environment has associated health risk concerns. Radon ( $^{222}\text{Rn}$ ) and thoron ( $^{220}\text{Rn}$ ) are radioactive gaseous elements produced as immediate decay products of  $^{226}\text{Ra}$  and  $^{232}\text{Th}$  respectively, found in decay chains of  $^{238}\text{U}$  and  $^{232}\text{Th}$  present in earth's crust. Radon having half-life ( $t_{1/2}$ ) of 3.8235 days decays by alpha radiation of energy 5.48 MeV where as thoron having half-life ( $t_{1/2}$ ) of 55.6 sec emits alpha radiation of energy 6.28 MeV. Radon has been long known as lung cancer causing agent (Darby et al., 2005; Stojanovska et al., 2011). Radon and thoron gases enter into the indoor air through the process of exhalation from soil and building materials (Nazaroff and Nero, 1988). These gases and their decay products present in air enter the human body mainly through inhalation. Recent studies have established that thoron

---

A. Kaushal (✉)  
Department of Physical Sciences, I.K.G. Punjab Technical University, Kapurthala 144601, Punjab, India  
e-mail: anjali13kaushal@gmail.com

A. Kaushal · N. Sharma  
Department of Physics, D.A.V. College, Jalandhar 144008, Punjab, India

M. Joshi  
Radiological Physics & Advisory Division, Bhabha Atomic Research Centre, Mumbai, India

A. Sarin  
Department of Physical Sciences, I.K.G. Punjab Technical University, Amritsar Campus, Amritsar 143105, Punjab, India

and its decay products also have significant contribution to inhalation dose along with radon and associated decay products (Smetsers & Thomas, 2019). Interaction of alpha particles, emitted by the short lived decay products of radon and thoron with biological tissues in the lungs may lead to DNA damage resulting in development of lung cancer (Edling et al., 1986; Sevc et al., 1976). The worldwide annual effective dose received by the population from all natural and artificial sources is 2.8 mSv, out of which nearly 85 % of the dose (2.4 mSv) comes from only natural background radiations (UNSEAR, 2000b). Also it is well documented that radon and thoron along with their decay products account for more than 50% of the natural background radiation dose received by the humans (UNSCEAR, 2008). The indoor concentration of radon, thoron and decay products depends on environmental (such as seasons) as well as anthropogenic factors (such as dwellings). Several studies have highlighted the role of such factors towards the variations of the indoor concentration data in the past. Stojanovska et al. (2011) in their study performed in dwellings of Macedonia found that the average radon concentration was highest (115 Bq/m<sup>3</sup>) in the winter season among winter, spring, summer and autumn seasons. They also studied the influence of building characteristics such as floor type, house age, building material, basement and type of windows on radon concentration. In a follow-up work in the same region, Stojanovska et al. (2013) obtained seasonal and regional variability for the measured data of indoor thoron concentration. A study performed in the region of Garhwal Himalayas (Ramola et al., 2016) revealed that ventilation conditions do not affect the thoron concentration but affect the radon concentration due to the shorter half-life of the former. The study also showed the dependency of radon/thoron, their decay products and equilibrium factors on seasons. The geometric mean annual effective dose due to radon and its decay products and thoron and its decay products was found to be 1.1 mSv and 0.5 mSv, respectively. Researchers have taken keen interest in the Punjab region in recent past aiming to measure and interpret indoor radon/thoron and the decay product's concentration levels. Mehra et al. (2006) reported an average indoor concentration value of 90.60 Bq/m<sup>3</sup> in their measurement campaign performed using the bare mode technique in the Malwa region of Punjab. Virk and Sharma (2000) reported variation of the annual effective dose from 0.61 to 1.11 mSv with an average value of 0.92 mSv

using a twin-chamber Rn-Tn dosimeter cup for Punjab. The annual effective dose has also been reported varying between 3 and 10 mSv for Hamirpur district, Himachal Pradesh (Singh et al., 2016). Widely varying geological influences, climatic patterns, source term etc. necessitate study of measurements of radon and thoron gases and decay products for different regions covering different contexts.

The present study measures the indoor concentration of radon/thoron and their decay products in Ludhiana district of Punjab, India. Pinhole dosimeters for gaseous measurements and deposition-based progeny sensors for decay product measurements have been used in this work. The measured values have been employed to estimate the equilibrium factors, inhalation doses and annual effective doses for this region. The work discusses interpretations of the observed data in terms of the effect of variations in seasons, building materials, ventilation condition, altitude etc. as well.

## Study area

### Geology

Ludhiana district is centrally located in the Malwa region (plain) of Punjab, India, as shown in Fig. 1. The total geographical area occupied by the district is about 3767 km<sup>2</sup>. In 2011, the total population was 3,498,739 in the district (District survey report). The district is situated between north latitudes 30° 33' and 31° 01' and east longitudes 75° 25' and 76° 27'. The area is covered by Indo-Gangetic alluvium. The variation in soil profile is sandy loam to clayey with normal reaction (pH 7.8 to 8.5) (Ludhiana district Punjab, 2013). Figure 1 is showing different types of soil in Punjab state of India (Punjab Remote Sensing Centre, Ludhiana) as well. The major hydrographic features of the district are Satluj river and its minor tributary, Budhanala.

### Climate

The climatic periods of district in a year are described as tropical steppe, hot and semi-arid. These are generally dry with hot summer and very cold in winter except the monsoon season. According to the District survey report, there are four seasons viz. winter

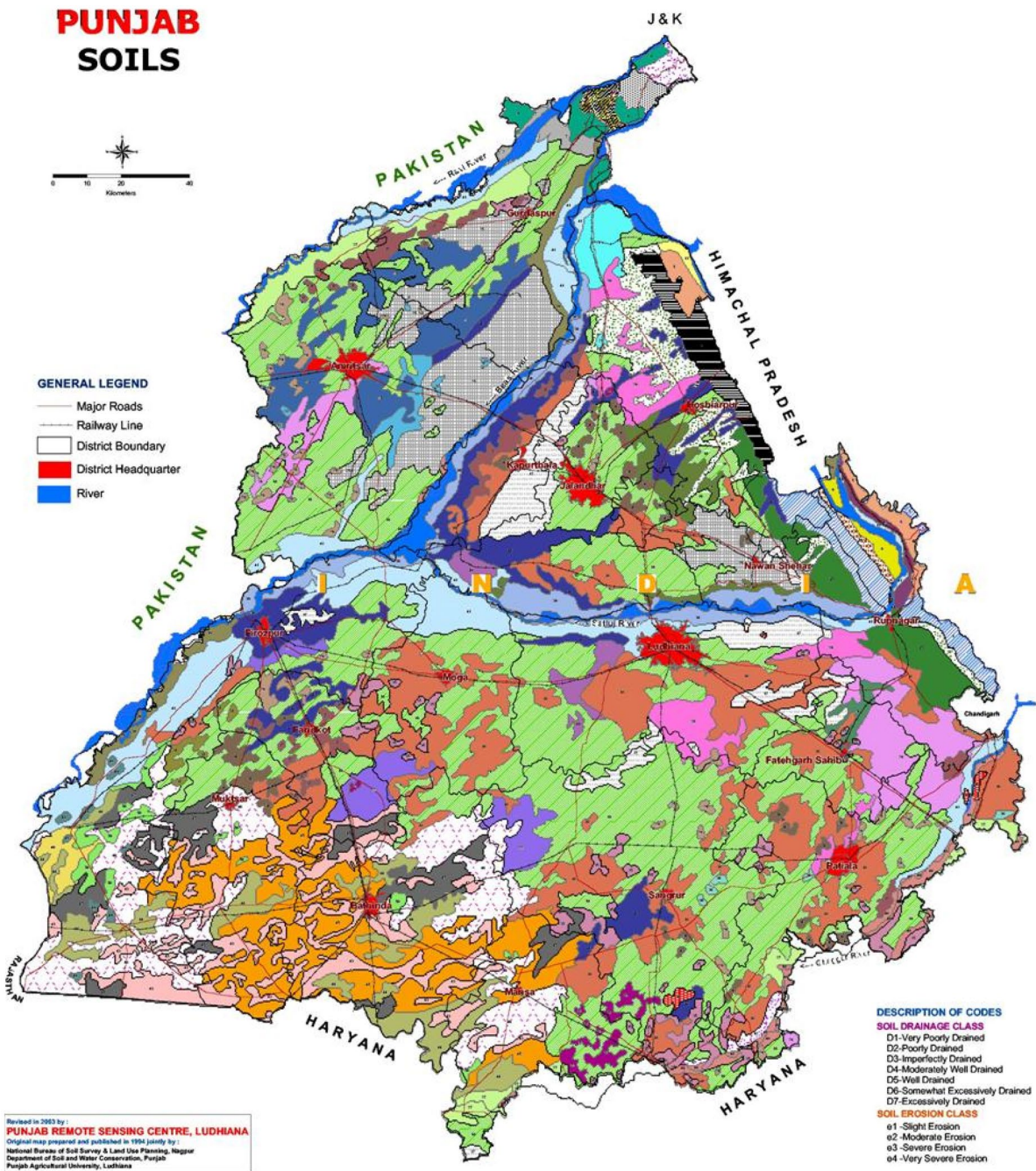


**Fig. 1** Map showing different soil types in Punjab state of India (Punjab Remote Sensing Centre, Ludhiana)

(mid-November to early March), summer (March to end of June), monsoon (July, August and first half of September) and post-monsoon (mid-September to mid-November). June is known to be the hottest month due to the mean daily temperature of 40.6 °C,

which reaches as high as 45 °C on single days. January is the coldest month with a mean minimum temperature of 6.4 °C. In August, the precipitation reaches the peak with average rainfall of 202 mm (District survey report).

**Table 1** Summary of dwelling characteristics

S. no	Parameters	Classification	Associated frequencies
1	Outdoor gamma level	< 0.1	101
		0.1–0.2	116
2	Room	Bedroom	53
		Hall	39
		Kitchen	14
3	Ventilation	Poor	21
		Average	31
		Good	54
4	Floor material	Mud	20
		Fired brick	17
		Cement	34
		Stone/marble	21
		Mosaic floor tile	14

## Materials and methods

### Design of the investigation

The main objective of the present study was to collect the representative results of levels of indoor radon/thoron and their decay products in the Ludhiana

district. A preliminary study was conducted in 217 villages of the district to measure the outdoor gamma dose rate levels. These measurements were carried out in air at a height of 1 m above the ground using an AT2140 portable dosimeter (ATOMTEX). These villages were then classified into three categories on the basis of gamma dose rate levels. The criterion for classification was the villages with gamma dose rate < 0.1  $\mu\text{Sv/h}$ , dose rate in range 0.1–0.2  $\mu\text{Sv/h}$  and villages with outdoor gamma dose rate level > 0.2  $\mu\text{Sv/h}$ . In our measurements, no villages with dose rate levels > 0.2  $\mu\text{Sv/h}$  were found. For these categories, dwellings were further divided on the basis of floor material like mud, fired bricks, mosaic floor tiles, cement and marble. Floor was chosen because soil beneath a dwelling is considered the most prominent source of indoor radon.

Table 1 shows the statistics of the dwellings chosen for the preliminary and the main part of the present study. Out of 217 samples, 106 dwellings from 42 villages were selected for the main part. Figure 2 depicts the location of 42 villages selected for conducting the measurements in study area. The targeted dwellings were also divided on the basis of ventilation criterion (good, average, poor) and type of room (bedroom, hall and kitchen).

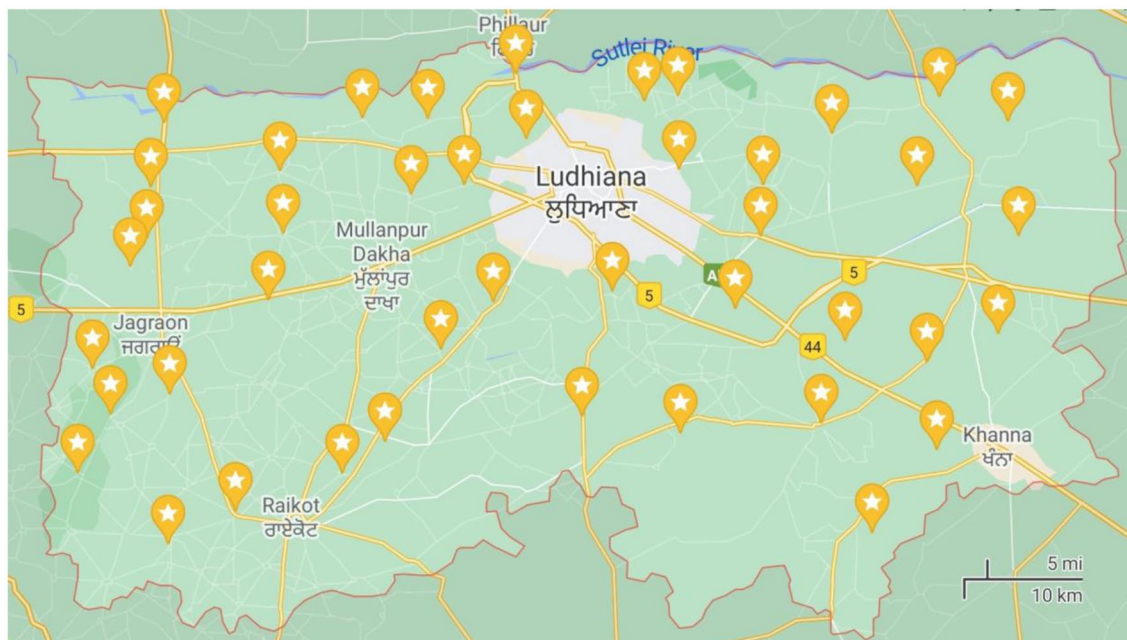


**Fig. 2** Map showing the location of 42 villages selected for measurements in Ludhiana district

**Table 2** Mean daily maximum and minimum temperatures, humidity and precipitation/rainfall in Ludhiana district of Punjab

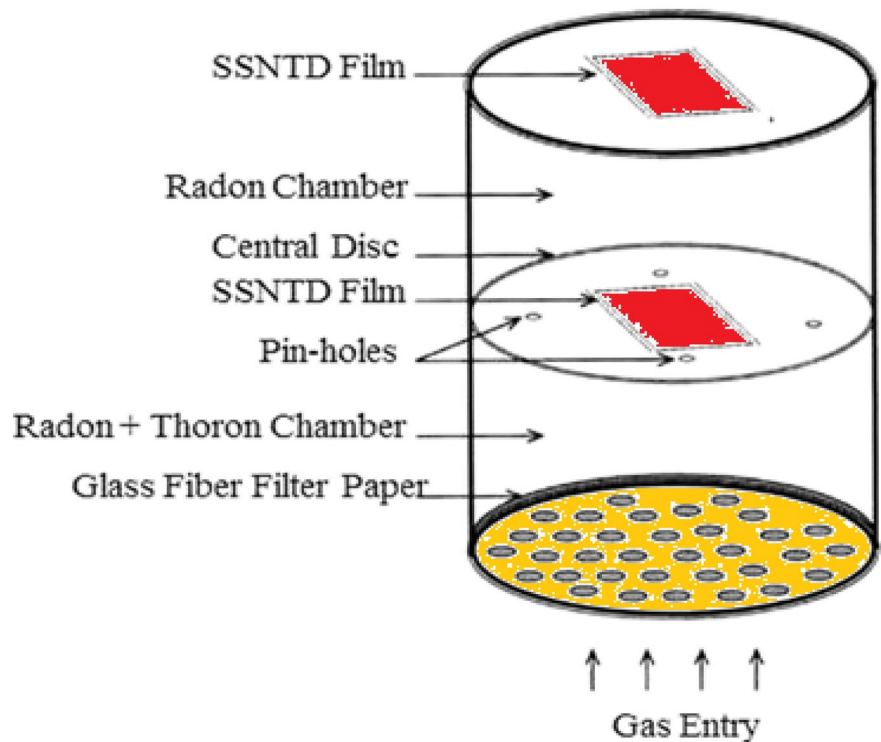
Months	Mean daily maximum temperature range (°C)	Mean daily minimum temperature range (°C)	Humidity range (%)	Precipitation/ rainfall range (mm)
March–June	28.6–40.6/36.3	13.6–27.2/21.1	22–38/31	8–52/27
July–October	33.6–36.2/34.9	17.4–26.8/23.6	34–64/52.5	26–202/136
Nov.–Feb	19.5–27.7/22.7	6.4–10.5/8.1	34–52/45.25	6–30/18.25

Measurements were conducted in three cycles of 4 months to include the effect of seasonal variation. These three cycles of months are chosen on the basis of temperature, humidity and precipitation/rainfall level as shown in Table 2 (District survey report). The three cycles of measurements were from November to February (winter season), March to June (summer season) and July to October (rainy season). Pre- and post-monsoon months were combined into rainy season as the mean daily maximum temperature for these months was close. High humidity in the months of July to October is due to higher precipitation in these months compared to months of other seasons.

Estimation of indoor radon and thoron gas concentrations

For the estimation of indoor radon and thoron gas concentrations, a single-entry (facing down) pinhole dosimeter (Fig. 3) comprising of SSNTD (solid-state nuclear track detector) LR-115 film was used. It gives time-integrated concentration levels of radon and thoron and is based on the radon-thoron discrimination technique. The minimum detection limit for radon and thoron concentration in the pinhole dosimeter is 2 Bq/m<sup>3</sup> and 6 Bq/m<sup>3</sup>, respectively (for details see, Sahoo et. al., 2013).

**Fig. 3** Schematic diagram of single-entry pinhole dosimeter



The dosimeters were suspended from the ceiling, at least 10–20 cm away from nearest wall and at a height of at least 1.5 m from the ground for an exposure period of 4 months. The retrieved films were chemically etched in the laboratory with 2.5 N NaOH at 60 °C for 90 min and counted using a spark counter to get the values of the density of tracks registered on the LR-115 films.

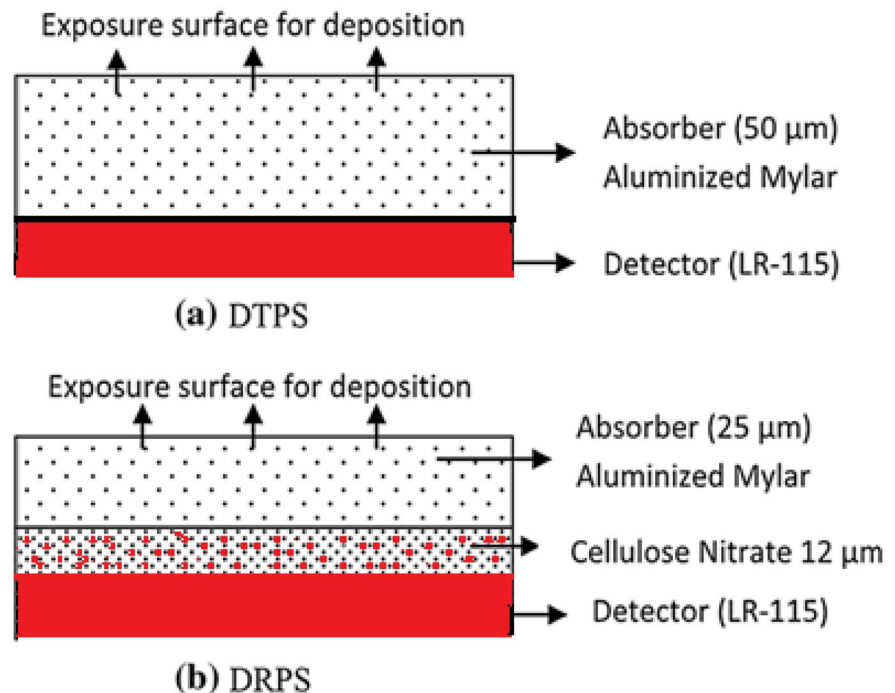
Radon and thoron gas concentrations were calculated from the track densities using the formulae given in Eqs. (1) and (2) (Sahoo et. al., 2013):

$$C_R = \frac{T_1 - B}{t \times K_R} \quad (1)$$

$$C_T = \frac{T_2 - T_1}{t \times K_T} \quad (2)$$

where  $C_R$  is the radon gas concentration ( $\text{Bq/m}^3$ );  $T_1$  and  $T_2$  are the track densities ( $\text{tracks/cm}^2$ ) measured for both the radon and radon + thoron chambers, respectively;  $B$  is the background counts observed;  $K_R$  ( $0.017 \pm 0.003 \text{ tracks/cm}^2/\text{day/Bq/m}^3$ ) and  $K_T$  ( $0.010 \pm 0.005 \text{ tracks/cm}^2/\text{day/Bq/m}^3$ ) are the calibration factors for radon in the radon chamber and for thoron in the radon + thoron chamber, respectively; and  $t$  is the exposure period (number of days).

**Fig. 4** Schematic diagram of direct deposition-based radon/thoron progeny sensors (DTPS/DRPS). (a) is for DTPS and (b) for DRPS



Estimation of equilibrium equivalent radon/thoron concentrations (*EERC/EETC*)

Measurements of equilibrium equivalent radon/thoron concentrations (*EERC/EETC*) were performed with direct radon/thoron progeny sensors (DRPS/DTPS), depicted in Fig. 4.

In the DRPS, an absorber of thickness 37 μm is in combination with the LR-115 detector, to detect α-particles emitted from  $^{214}\text{Po}$  having energy of 7.69 MeV, formed from the decay of  $^{218}\text{Po}$ ,  $^{214}\text{Pb}$  and  $^{214}\text{Bi}$  atoms deposited on the sensor (Mishra et. al., 2009). To measure *EETC*, the LR-115 detector is mounted with an aluminised Mylar absorber of 50-μm thickness to record the tracks formed by α-particles emitted from  $^{212}\text{Po}$  having energy of 8.78 MeV, which are formed from the decay of  $^{212}\text{Pb}$  and  $^{212}\text{Bi}$  atoms deposited on the Mylar surface. Due to difference in thickness (50 μm and 37 μm) of the absorber in the DTPS and DRPS, there is no mutual interference of deposited progenies. In the DRPS and DTPS, the minimum detection limit for radon progeny and thoron decay products is 1  $\text{Bq/m}^3$  and 0.1  $\text{Bq/m}^3$ , respectively (Bangotra et. al., 2019). The DRPS and DTPS were exposed along with the pinhole dosimeters in the dwellings for the same exposure period. The exposed LR-115 films were chemically etched and counted as explained earlier.

The equilibrium equivalent thoron/radon concentrations (*EETC/EERC*) were calculated using the formulae given by Eqs. (3) and (4) (Mishra and Mayya, 2008):

$$EETC = \frac{T_T - B}{t \times S_{TT}} \tag{3}$$

$$EERC = \frac{(T_R - B) - EETC \times S_{RT} \times t}{t \times S_{RR}} \tag{4}$$

where  $S_{TT}$ ,  $S_{RT}$  and  $S_{RR}$  are sensitivity factors for DTPS and DRPS, respectively, estimated by Mishra et al. (2010). The value of the sensitivity factor  $S_{TT}$  is  $0.94 \pm 0.027$  tracks/cm<sup>2</sup>/day/*EETC* (Bq/m<sup>3</sup>), and sensitivity factors  $S_{RR}$  and  $S_{RT}$  are  $0.09 \pm 0.0036$  tracks/cm<sup>2</sup>/day/*EERC* (Bq/m<sup>3</sup>).  $B$  is the background track density;  $T_T$  and  $T_R$  are the measured track densities in DTPS and DRPS, respectively; and  $t$  is exposure period (number of days).

Estimation of equilibrium factors

Significant dependence of equilibrium factors on the regions, climate, ventilation and other factors has been reported in different studies (Ramola et. al., 2016, Porstendorfer, 1984). Hence, the equilibrium factors were computed using the gas concentrations and the progeny concentrations for individual dwellings. For calculating

equilibrium factors, i.e.  $F_R$  for radon and  $F_T$  for thoron, the following Eqs. (5) and (6) were used:

$$F_R = \frac{EERC}{C_R} \tag{5}$$

$$F_T = \frac{EETC}{C_T} \tag{6}$$

where  $C_R$  and  $C_T$  are radon and thoron concentrations measured from pinhole twin cup dosimeters, respectively. *EETC/EERC* are the equilibrium equivalent concentrations of thoron and radon calculated from direct thoron/radon progeny sensors, i.e. DTPS/DRPS, respectively.

Estimation of total annual inhalation dose

The annual inhalation dose due to radon/thoron and their decay products was calculated by using Eq. (7) (UNSCEAR, 2000b):

$$D(\text{mSv/year}) = (C_R \times 0.17 + C_T \times 0.11 + EERC \times 9 + EETC \times 40) \times 8760 \times 0.8 \times 10^{-6} \tag{7}$$

where  $0.17/0.11/9/40$  nSv (Bqh/m<sup>3</sup>)<sup>-1</sup> are dose conversion factors for radon gas/thoron gas/radon decay products/thoron decay products, respectively (UNSCEAR, 2000a); 8760 h/year is the indoor occupancy time; and

**Table 3** Measured values of indoor radon/thoron, equilibrium equivalent concentrations (*EERC/EETC*), equilibrium factors ( $F_R/F_T$ ) and annual inhalation dose and annual effective doses (*AEDR/AEDT*)

	$C_R$ (Bq/m <sup>3</sup> )	$C_T$ (Bq/m <sup>3</sup> )	<i>EERC</i> (Bq/m <sup>3</sup> )	<i>EETC</i> (Bq/m <sup>3</sup> )	$F_R$	$F_T$	Dose (mSv/y)	<i>AEDR</i> (mSv/y)	<i>AEDT</i> (mSv/y)
<i>Min</i>	9.4±1.6	11.4±3.1	2.9±0.5	0.2	0.13	0.003	0.3	0.2	0.1
<i>Max</i>	43.4±4.7	145±11	17.8±1.3	1.5±0.1	0.81	0.061	1.6	1.1	0.4
<i>Avg</i>	22.7±3.2	49.2±6.1	9.3±0.9	0.6±0.1	0.47	0.021	0.8	0.6	0.2
<i>GM</i>	21.7	44.9	8.8	0.6	0.45	0.018	0.8	0.5	0.2
<i>SD</i>	6.9	21.1	3.2	0.3	0.13	0.013	0.3	0.2	0.1
<i>GSD</i>	1.4	1.6	1.4	1.6	1.36	1.82	1.4	1.4	1.6
<i>1<sup>st</sup>Quart</i>	17.9	33.9	6.8	0.4	0.38	0.012	0.6	0.4	0.1
<i>Med</i>	21.6	47.2	9.5	0.5	0.46	0.018	0.8	0.6	0.2
<i>3<sup>rd</sup>Quart</i>	27.1	61.5	11.2	0.8	0.54	0.026	1.0	0.7	0.2
<i>IQR</i>	9.2	27.7	4.5	0.4	0.16	0.014	0.4	0.3	0.1
<i>Skew</i>	0.5	1.2	0.4	1.0	0.13	1.209	0.02	0.4	1.0
<i>Kurt</i>	0.2	3.4	-0.2	0.5	-0.1	1.094	0.4	-0.2	0.5

*Min* minimum, *Max* maximum, *Avg* average, *GM* geometric mean, *SD* standard deviation, *GSD* geometric standard deviation, *1<sup>st</sup>Quart* 1st quartile, *Med* median, *3<sup>rd</sup>Quart* 3rd quartile, *IQR* interquartile range, *Skew* skewness, *Kurt* kurtosis

0.8 is the indoor occupancy factor;  $10^{-6}$  is the multiplication factor used for conversion of nanosieverts to millisieverts.

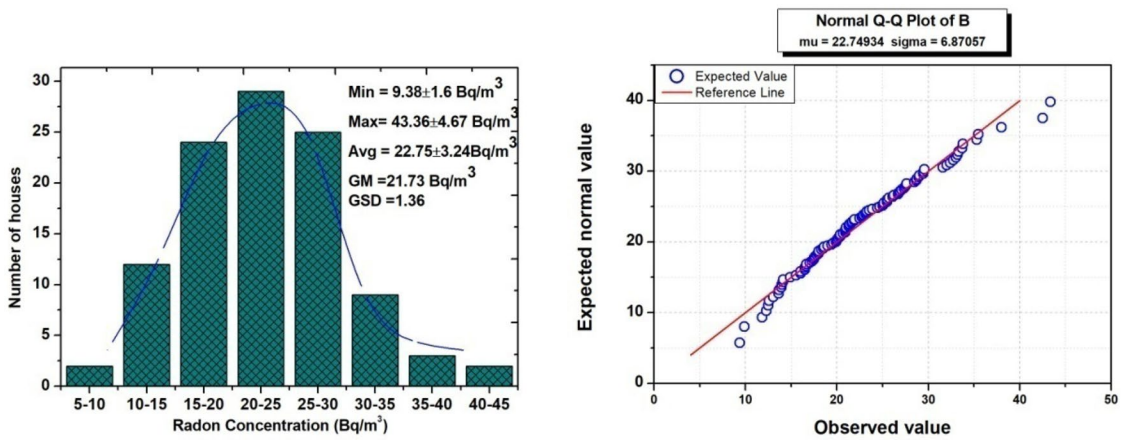
**Results and discussion**

Statistical interpretation of overall annual results

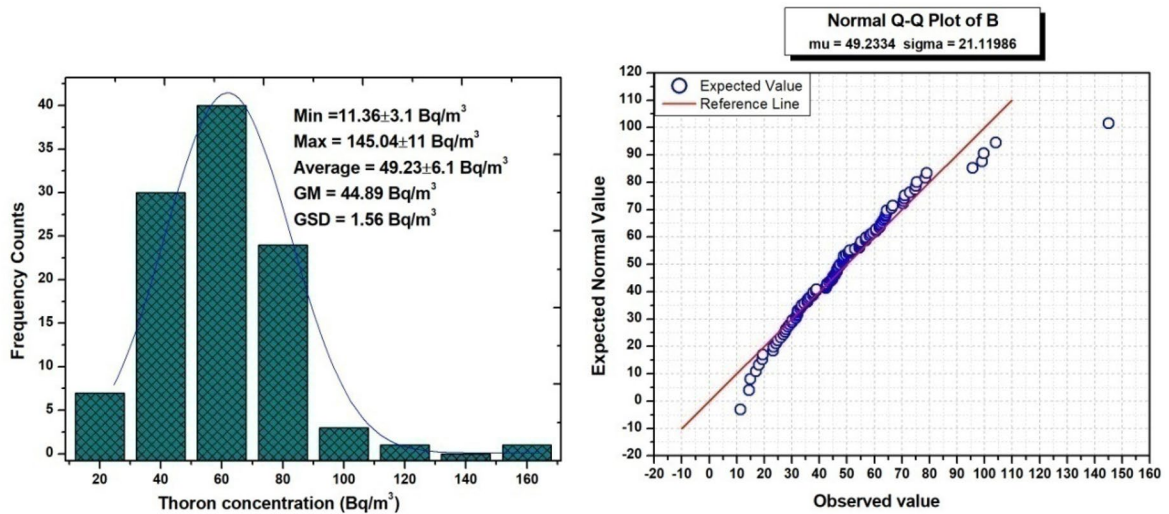
Annual average concentrations of radon, thoron and their decay products along with their descriptive

statistics are summarised in Table 3. The radon concentration ( $C_R$ ) varied from  $9.4 \pm 1.6$  to  $43.4 \pm 4.7$  Bq/m<sup>3</sup> with an average of  $22.7 \pm 3.2$  Bq/m<sup>3</sup>, and the thoron concentration ( $C_T$ ) varied from  $11.4 \pm 3.1$  to  $145 \pm 11$  Bq/m<sup>3</sup> with an average of  $49.2 \pm 6.1$  Bq/m<sup>3</sup>. The frequency distribution and quartile-quartile (Q-Q) plot for radon and thoron data are shown in Fig. 5a, b, respectively.

In Fig. 5a, the Q-Q plot for radon concentration (right) is showing that both ends deviate from the



(a) (left) Frequency distribution and (right) Q-Q plot for annual average radon concentration



(b) (left) Frequency distribution and (right) Q-Q plot for annual average thoron concentration

**Fig. 5** a Frequency distribution (left) and Q-Q plot (right) for annual average radon concentration. b Frequency distribution (left) and Q-Q (right) plot for annual average thoron concentration



straight line but the middle points follow a straight line. This verifies that the distribution is log-normal distribution (Fig. 5a) (left)). Skewness (0.5) and kurtosis (0.2) are showing that the distribution is fairly symmetric and light tailed, respectively (Table 3), and the histogram is positively skewed.

The Q-Q plot (right) and frequency distribution (left) for the data of thoron concentration are shown in Fig. 5b. Similar to radon, deviations observed in the Q-Q plot and skewness and kurtosis values for thoron concentration data (Table 3) indicate that the distribution is log normal in nature. The measured average *EERC* ranged between  $2.9 \pm 0.5$  and  $17.8 \pm 1.3$  Bq/m<sup>3</sup> with an average of  $9.3 \pm 0.9$  Bq/m<sup>3</sup>, and the average *EETC* ranged between 0.2 and  $1.5 \pm 0.1$  Bq/m<sup>3</sup> with an average of  $0.6 \pm 0.1$  Bq/m<sup>3</sup>. The frequency distribution for *EERC* and *EETC* data is depicted by Q-Q plots in Fig. 6a, b, respectively. The Q-Q plot for annual average *EERC* (Fig. 6a) shows that the data is symmetric with skewness 0.4 and light tailed with kurtosis -0.2. Similarly, Fig. 6b shows that annual average *EETC* distribution is moderately skewed with skewness 1.0 and light tailed with kurtosis 0.5.

The reason for the observed variations in the data could be attributed to the difference in the geological condition of sampling sites, ventilation condition of the houses and building material used for the construction. The annual average thoron concentration has been found higher in comparison to the annual

average radon concentration, similar to the trend of data seen in Kumar et al. (2017). The geometric mean values of annual average indoor concentrations of radon, thoron, *EERC* and *EETC* (with geometric standard deviations in brackets) were obtained to be 21.73 Bq/m<sup>3</sup> (1.4), 44.89 Bq/m<sup>3</sup> (1.6), 8.76 Bq/m<sup>3</sup> (1.4) and 0.58 Bq/m<sup>3</sup> (1.6), respectively. For indoor radon, 25% (1st quartile) of data lies below 17.9 Bq/m<sup>3</sup> and 75% (3rd quartile) of data lies below 27.1 Bq/m<sup>3</sup> with a median value of 21.6 Bq/m<sup>3</sup>. For indoor thoron, 25% (1st quartile) of data lies below 33.9 Bq/m<sup>3</sup> and 75% (3rd quartile) of data lies below 61.5 Bq/m<sup>3</sup> with a median value of 47.2 Bq/m<sup>3</sup>. *EERC* has 25% (1st quartile) of data below 6.8 Bq/m<sup>3</sup> and 75% (3rd quartile) below 11.2 Bq/m<sup>3</sup> with median 9.5 Bq/m<sup>3</sup>, while 25% of *EETC* (1st quartile) data is below 0.4 Bq/m<sup>3</sup> and 75% (3rd quartile) is below 0.8 Bq/m<sup>3</sup> with a median value of 0.5 Bq/m<sup>3</sup>.

The measured values of radon and thoron concentrations are within the safe limit of 300 Bq/m<sup>3</sup> recommended by ICRP (2011). The estimated annual average concentration of radon (22.7 Bq/m<sup>3</sup>) was also found to be lower than the global average value of 40 Bq/m<sup>3</sup> and the national average of 42 Bq/m<sup>3</sup> (UNSCEAR, 2000a and Mishra et al., 2009). In contrast, the thoron (49.2 Bq/m<sup>3</sup>) concentration was found to be higher than the global average value of 10 Bq/m<sup>3</sup> as well as the national average value of 12.2 Bq/m<sup>3</sup> (UNSCEAR, 2000a and Mishra et al.,

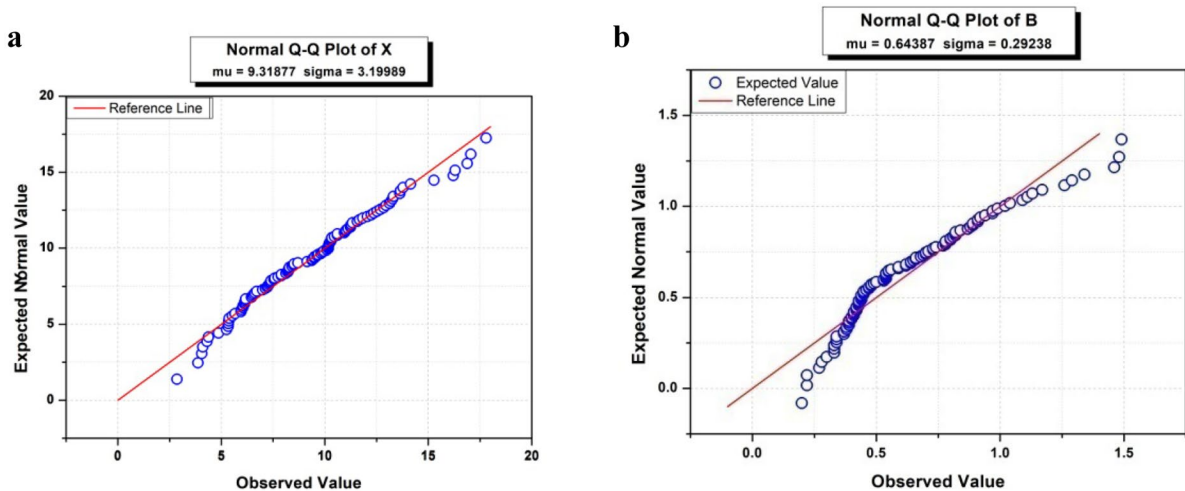


**Fig. 6** **a** Frequency distribution of annual average radon progeny concentration (*EERC*) and **b** thoron progeny concentration (*EETC*) (Bq/m<sup>3</sup>)

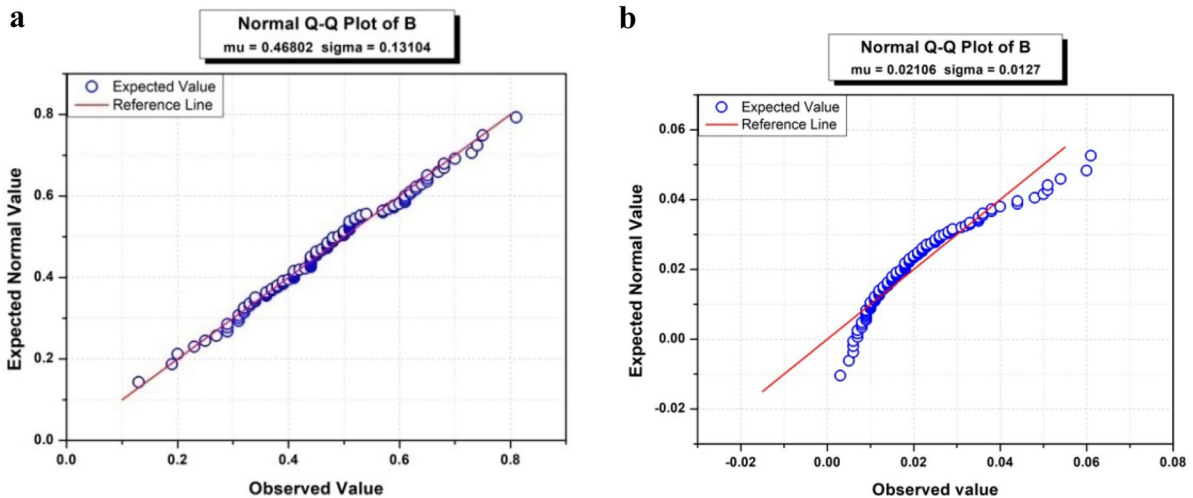


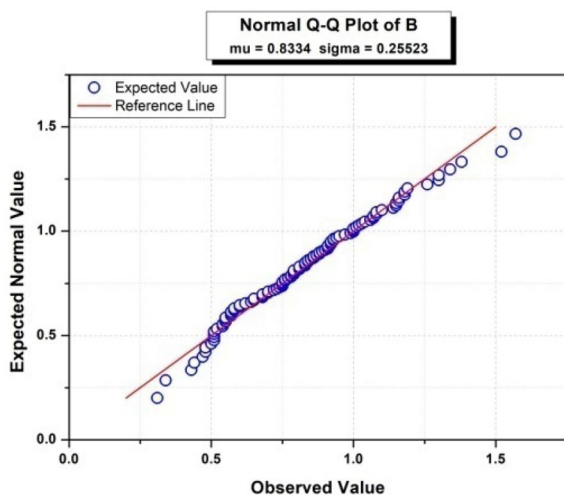
**Fig. 7** **a** Frequency distribution of annual average radon equilibrium factor and **b** thoron equilibrium factor

2009). The higher thoron in the study region could be due to the higher thorium content in the source term. The annual average equilibrium factor for radon was found to vary from 0.13 to 0.81 with an average of 0.47. The frequency distribution of the equilibrium factor of yearly averaged radon and its decay products is shown in Fig. 7a. Here, the distribution is normal distribution with a *GM* of 0.45 (*GSD* 1.36). The calculated average value of the equilibrium factor for radon and its decay products (0.47) has been found to be slightly higher than the global average

value (UNSCEAR (2008)). The equilibrium factor evaluated for thoron ranged between 0.003 and 0.061 with an average of 0.021. Log-normal distribution has been found for the equilibrium factor of yearly averaged thoron and its decay products, which is shown in the frequency distribution graph in Fig. 7b. The average value (0.021) has been found to be smaller compared with the global average value of 0.1 (UNSCEAR, 1993). Variations in equilibrium factors and the reasons for the same have been discussed elsewhere (Porstendorfer, 1984; Jilek et al., 2010; Yu & Nikezic, 1996; Ramola et al., 2003, 2016).

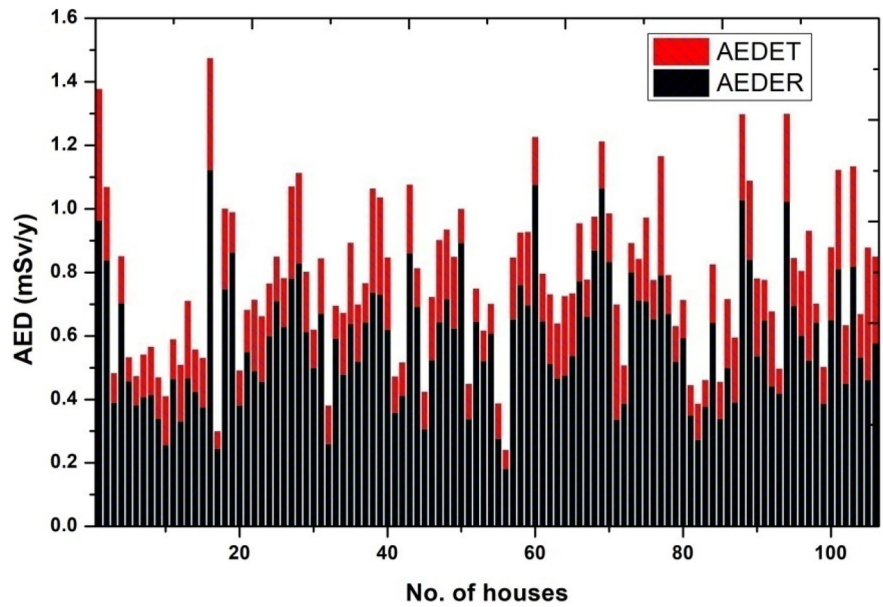
The calculated values of the annual average inhalation dose due to radon, thoron and their decay products has been found to vary from 0.3 to 1.6 mSv with an average of 0.8 mSv. The geometric mean value of the annual average inhalation dose was found to be 0.8 with *GSD* 1.4. Normal distribution of the data has been seen in the frequency distribution graph (Fig. 8). The annual average value measured is less than the world's average inhalation dose of 1.2 mSv given by UNSCEAR (2000b).

The annual average effective doses due to radon and thoron decay products have been found to vary from 0.2 to 1.1 mSv with an average of 0.6 mSv and 0.1 to 0.4 mSv with an average of 0.2 mSv, respectively. Figure 9 shows the contribution of the total annual effective dose due to radon and thoron decay products. It can be seen that 75% and 25% of the annual average effective dose were contributed by radon and thoron decay products, respectively, for



**Fig. 8** Frequency distribution for total inhalation dose

**Fig. 9** Total annual effective dose due to radon and thoron progenies



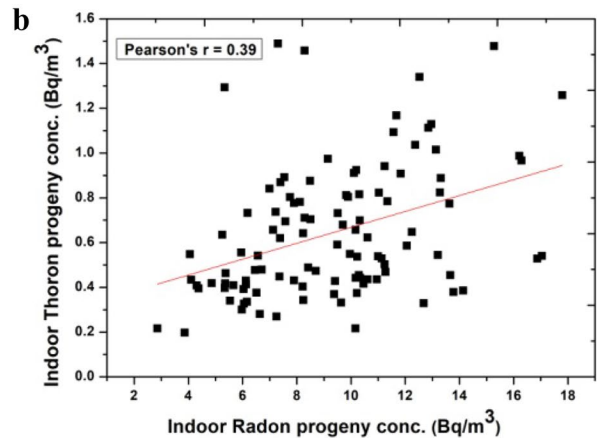
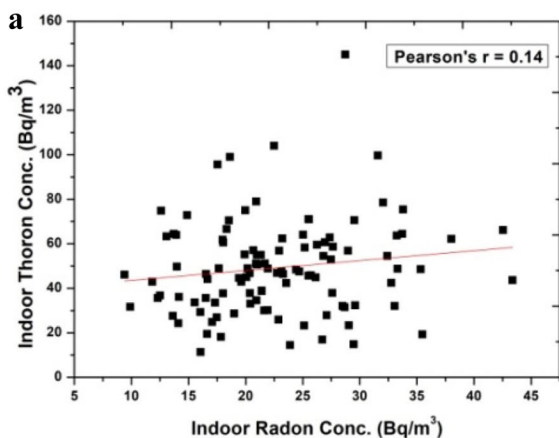
the study region. This shows the importance of decay product measurements for the study region.

Figure 10a represents the correlation plot for measured indoor radon and thoron concentration data while Fig. 10b shows a similar plot for measured radon and thoron decay product concentrations. As can be seen, a weak positive correlation ( $r=0.14$ ) was obtained for the gaseous measurement data whereas a low moderate positive correlation ( $r=0.39$ ) was obtained for the decay product concentrations. A positive moderate correlation with  $r$  values of 0.52

and 0.41 was obtained for the pairs radon gas-radon decay product concentration (Fig. 11a) and thoron gas-thoron gas concentration data (Fig. 11b), respectively. No correlation ( $r=0.01$ ) was obtained between equilibrium factors of radon and thoron (Fig. 12).

Seasonal dependence of indoor radon/thoron and progeny concentrations

As mentioned earlier, the yearlong investigation was carried out in three cycles of 4 months to study



**Fig. 10** **a** Correlation between annual indoor radon and thoron concentrations and **b** annual indoor radon progeny and thoron progeny concentrations.

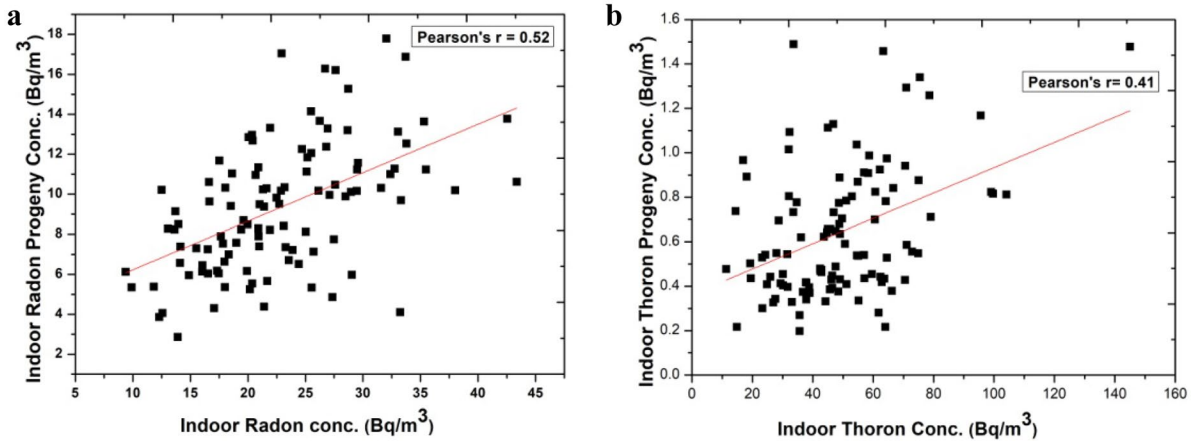


**Fig. 11** **a** Correlation between annual indoor radon and radon progeny concentrations and **b** annual indoor thoron and thoron Progeny concentrations.

the seasonal dependence of radon/thoron and decay product concentration. Detailed statistically estimated parameters of seasonal variation can be seen in Table 4, and the variation with respect to different seasons is shown as box whisker plots in Fig. 13. Measurements revealed that radon and thoron show a similar trend of seasonal variation as shown in Doi et al. (1994) and Mishra et al., (2004). Radon/thoron and radon decay product (*EERC*) concentrations have been found higher in the winter season (Fig. 13; Table 4). In the winter season, the geometric mean values of annual average indoor concentrations of radon, thoron, *EERC* and *EETC* (with geometric standard deviations in brackets) were obtained to be 26.6 Bq/

$m^3$  (1.5), 45.2 Bq/ $m^3$  (2.2), 9.5 Bq/ $m^3$  (1.6) and 0.5 Bq/ $m^3$  (2), respectively. The values for equilibrium factors ( $F_R/F_T$ ), annual inhalation dose and annual effective doses (*AEDER/AEDET*) are also summarised in Table 4.

The skewness values of radon, thoron and *EERC* are 0.9, 0.6 and 1 for the winter season, respectively. These values indicate that the distribution of the data is moderately skewed. For *EETC*, the skewness value of 1.3 shows highly skewed data. The kurtosis values for radon (1.4), thoron (-0.2), *EERC* (0.5) and *EETC* (2.8) are less than 3, which indicates that the data is light tailed (Table 4).

In the winter season, due to cold weather, dwellers tend to keep the doors and windows mostly closed to increase the room temperature. Less ventilation leads to an increase in the concentration of radon/thoron gases in the room. Temperature inversion resulting in the trapping of gases near the surface also results in a high concentration in the winter season (Sathish et al., 2012; Sesana et al., 2003). The other reason may be the decrease in atmospheric pressure inside the rooms as compared to that outside, which increases the exhalation rate from the floor and walls (Mishra et al., 2004). For the study region, the radon gas concentration measured in 19% of dwellings was found to be higher than 40 Bq/ $m^3$  in the winter season. Similarly, for the case of thoron gas, the concentration in 14% of dwellings was measured to be above 100 Bq/ $m^3$  (Table 4). Measured values of indoor radon, thoron,

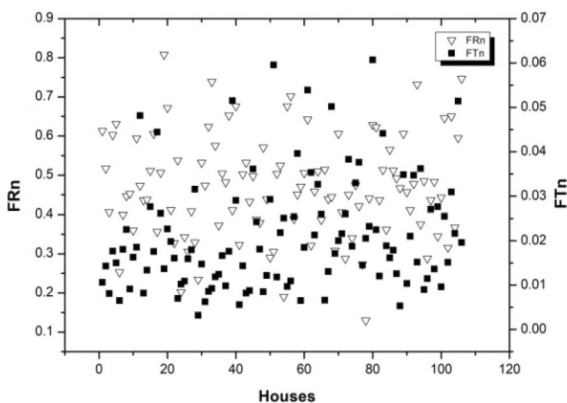


**Fig. 12** Variation of equilibrium factors of radon/thoron in dwellings of Ludhiana district

**Table 4** Seasonal variation in statistical measured values of indoor radon/thoron, equilibrium equivalent concentrations ( $EERC/EETC$ ), equilibrium factors ( $F_R/F_T$ ), annual inhalation dose and annual effective doses ( $AEDER/AEDET$ )

Season	$C_R$ , Bq/m <sup>3</sup>	$C_T$ , Bq/m <sup>3</sup>	$EERC$ , Bq/m <sup>3</sup>	$EETC$ , Bq/m <sup>3</sup>	$F_R$	$F_T$	Dose, mSv/y	$AEDER$ , mSv/y	$AEDET$ , mSv/y
Winter	Min	7.3	4	3.1	0	0	0.3	0.2	0
	Max	77.3	163.8	24.1	1.9	0.85	0.086	1.5	0.5
	Avg	29.1	57.5	10.5	0.5	0.4	0.015	0.9	0.2
	GM	26.6	45.2	9.5	0.5	0.36	0.01	0.8	0.1
	SD	12.3	35.1	4.8	0.3	0.19	0.016	0.3	0.1
	GSD	1.5	2.2	1.6	2	164	2.58	1.5	2
	1 <sup>st</sup> Quart	20.8	29.2	7.4	0.3	0.25	0.005	0.7	0.1
	Med	27.3	54.2	9.2	0.5	0.36	0.011	0.8	0.1
	3 <sup>rd</sup> Quart	35.1	80.2	12.5	0.7	0.48	0.018	1.1	0.2
	IQR	14.3	51	5.2	0.4	0.23	0.012	0.4	0.1
	Skew	0.9	0.6	1	1.3	0.87	2.312	0.8	0.3
	Kurt	1.4	-0.2	0.5	2.8	0.05	5.891	0.2	0.5
	Min	0.4	1.8	0	0	0	0	0	0
	Max	71.9	153.6	20.9	2.8	0.87	0.119	1.7	1.3
Summer	Avg	21	44.3	8.8	0.7	0.48	0.025	0.8	0.2
	GM	17.3	34.3	6.6	0.5	0.38	0.015	0.7	0.1
	SD	11.8	29.1	4.8	0.5	0.25	0.026	0.4	0.1
	GSD	2.1	2.2	3.1	3.2	2.42	3.421	2	3.2
	1 <sup>st</sup> Quart	12.2	17.4	5.4	0.4	0.28	0.008	0.5	0.1
	Med	20.7	40.6	8.5	0.6	0.47	0.015	0.8	0.2
	3 <sup>rd</sup> Quart	25.8	63.7	12.1	0.9	0.71	0.029	1.1	0.3
	IQR	13.6	46.3	6.6	0.6	0.43	0.021	0.6	0.2
	Skew	1.1	0.9	0.2	1.4	0.08	1.701	0.2	0.2
	Kurt	2.5	0.9	-0.5	3.1	-1.13	2.331	-0.4	-0.5
	Min	0.4	1.8	0	0	0	0	0	0
	Max	71.9	153.6	20.9	2.8	0.87	0.119	1.7	1.3
	Avg	21	44.3	8.8	0.7	0.48	0.025	0.8	0.5
	GM	17.3	34.3	6.6	0.5	0.38	0.015	0.7	0.4
SD	11.8	29.1	4.8	0.5	0.25	0.026	0.4	0.3	
GSD	2.1	2.2	3.1	3.2	2.42	3.421	2	3.1	
1 <sup>st</sup> Quart	12.2	17.4	5.4	0.4	0.28	0.008	0.5	0.3	
Med	20.7	40.6	8.5	0.6	0.47	0.015	0.8	0.5	
3 <sup>rd</sup> Quart	25.8	63.7	12.1	0.9	0.71	0.029	1.1	0.8	
IQR	13.6	46.3	6.6	0.6	0.43	0.021	0.6	0.4	
Skew	1.1	0.9	0.2	1.4	0.08	1.701	0.2	0.2	
Kurt	2.5	0.9	-0.5	3.1	-1.13	2.331	-0.4	-0.5	

**Table 4** (continued)

Season	$C_R$ , Bq/m <sup>3</sup>	$C_T$ , Bq/m <sup>3</sup>	$EERC$ , Bq/m <sup>3</sup>	$EETC$ , Bq/m <sup>3</sup>	$F_R$	$F_T$	Dose, mSv/y	$AE/DER$ , mSv/y	$AE/DET$ , mSv/y
Rainy									
<i>Min</i>	2.2	3.2	0.4	0	0.02	0.001	0.1	0	0
<i>Max</i>	66.3	187.4	20.9	2.4	0.9	0.099	1.9	1.3	0.7
<i>Avg</i>	18	44.3	8.5	0.7	0.52	0.023	0.8	0.5	0.2
<i>GM</i>	15.4	32.8	7	0.5	0.45	0.015	0.7	0.4	0.1
<i>SD</i>	9.8	31.7	4.6	0.5	0.23	0.022	0.4	0.3	0.1
<i>GSD</i>	1.8	2.4	2	2.2	1.91	2.561	1.7	2	2.2
<i>1<sup>st</sup>Quart</i>	11.3	17.8	5.6	0.4	0.34	0.008	0.5	0.4	0.1
<i>Med</i>	16.7	43	7.7	0.5	0.53	0.014	0.7	0.5	0.2
<i>3<sup>rd</sup>Quart</i>	22.4	56.3	11.3	0.8	0.74	0.034	1	0.7	0.2
<i>IQR</i>	11.1	38.5	5.8	0.4	0.4	0.026	0.5	0.4	0.1
<i>Skew</i>	1.5	1.4	0.7	1.7	-0.18	1.51	1	0.7	1.7
<i>Kurt</i>	5	3.4	0.2	3	-1.11	1.863	1	0.2	3

*Min* minimum, *Max* maximum, *Avg* average, *GM* geometric mean, *SD* standard deviation, *GSD* geometric standard deviation, *1<sup>st</sup>Quart* 1st quartile, *Med* median, *3<sup>rd</sup>Quart* 3rd quartile, *IQR* interquartile range, *Skew* skewness, *Kurt* kurtosis

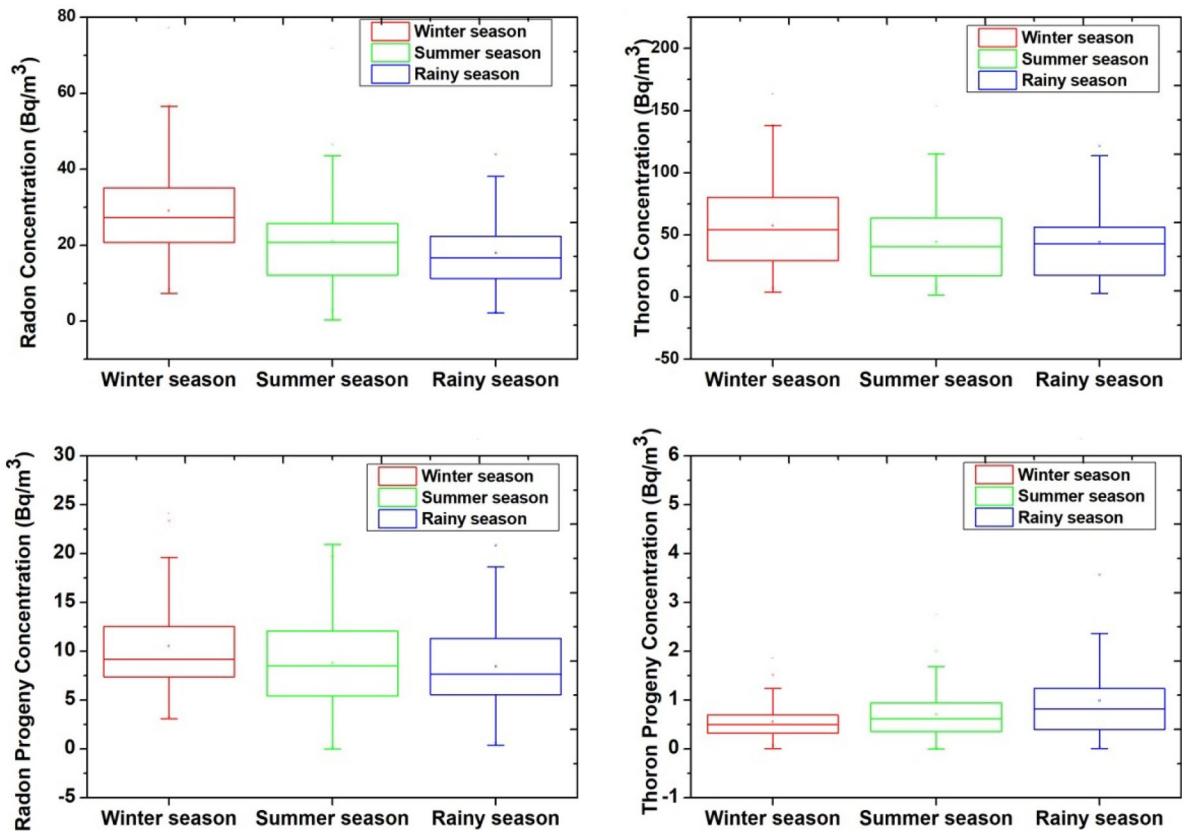


**Fig. 13** Box whisker plots showing seasonal dependence of radon, thoron and progeny concentrations (Bq/m<sup>3</sup>)

radon decay product and thoron decay product concentrations have been found to be nearly the same for rainy and summer seasons (Table 4). The reason behind it may be the similar ventilation conditions of the room for both seasons. The average thoron decay product concentration has been found to be nearly the same in all seasons as 1.9 Bq/m<sup>3</sup> (rainy), 1.9 Bq/m<sup>3</sup> (winter) and 1.8 Bq/m<sup>3</sup> (summer) (Table 4). The same trend of data can be seen in Omori et al. (2016) and Zhuo et al. (2000).

**Impact of building materials**

With a view to study the impact of building materials on indoor concentrations of gases and decay products, all the dwellings were divided into different categories as shown in Table 2. Division of dwellings for analysis was made on the basis of different types of floor, roof and wall material (Figs. 14 and 15a, b).

Out of 106 dwellings, approximately 90% of dwellings had brick walls with cement plastering, 50% of

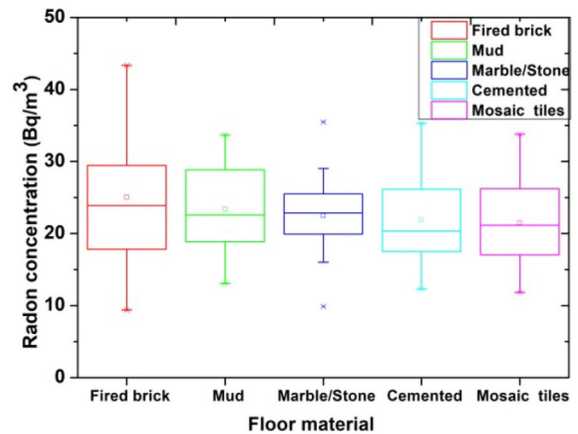


**Fig. 14** Radon concentration variation due to different floor materials

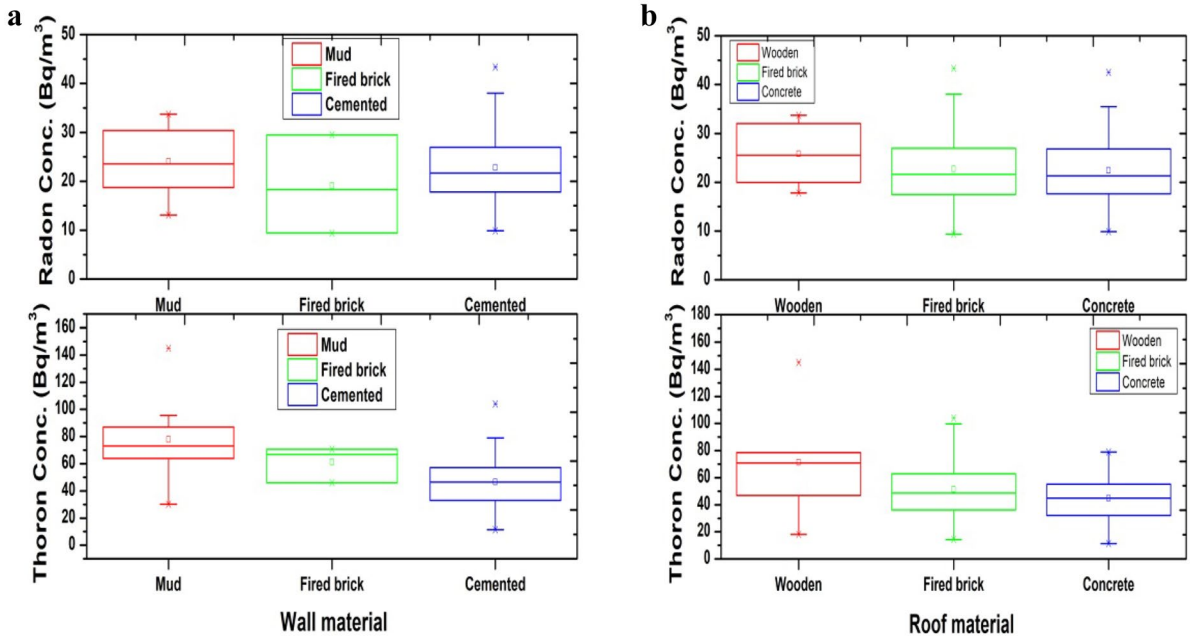


**Fig. 15** Radon and thoron concentrations due to **a** different wall materials and **b** different roofs

dwellings had an RCC (reinforced concrete construction) roof and 32% had a cemented floor. Studies of Ningappa et al. (2008) and Sannappa et al. (2003) have revealed that the indoor radon concentration is mainly dependent on the building materials used for construction, ventilation condition of the house and types of soil beneath.

In the present study, a higher concentration of indoor radon has been found in dwellings with fired brick and mud-plastered floors. As fired bricks are also made from the local soil, both mud and fired bricks are major contributors of indoor radon concentration (Fig. 14). The higher concentration for these floors might be due to usage of radium-rich soil in mud plastering (UNSCEAR, 1988) and high porosity (Ningappa et al., 2008). On the other extreme, the lower porosity of mosaic tiles resulted in a lower radon concentration (Fig. 14).

This investigation revealed that most of the roofs were made up of wooden/thatched, bricks and RCC materials. A higher radon/thoron concentration has been found in wooden/thatched roof houses, and a lower concentration has been found in RCC roof houses (Fig. 15b).

Figure 16 demonstrates that roof/wall combinations of different building materials have significant impact on the thoron concentration found in the room. As detectors were deployed near walls and roofs,

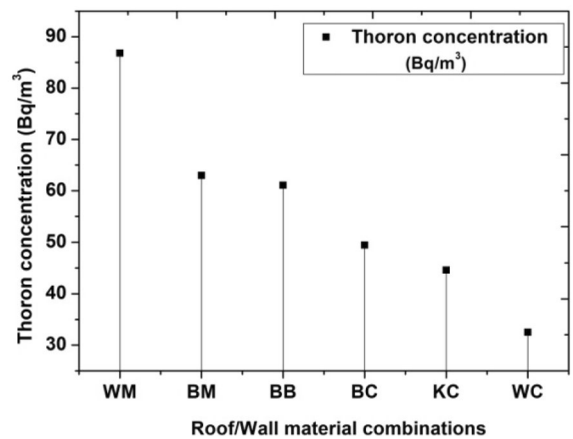
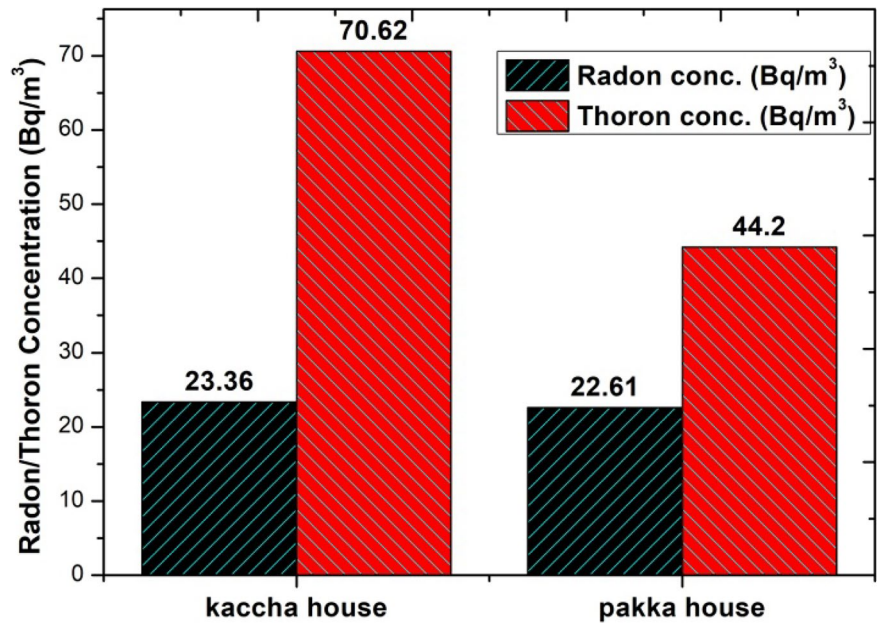


**Fig. 16** Thoron concentration variation among different roof and wall combinations. WM wooden roof/mud wall, BM fired brick roof/mud wall, BB fired brick roof and wall, BC fired brick roof/cemented wall, KC RCC roof/cemented wall, WC wooden roof/cemented wall



**Fig. 17** Radon/thoron concentration in kaccha and pakka houses



these were the main contributor of thoron gas rather than the floor due to the short half-life of thoron.

Footprints of mud-plastered walls can be seen in both combinations with wooden and brick roofs as wooden roof, mud and fired brick floors have shown a high concentration of thoron in the room figured out earlier. The fired brick roof and wall combination closely resembles fired brick roof and mud wall combinations as these bricks are also made with the thorium-rich local soil (UNSCEAR, 1988). Combinations of fired brick roof, RCC roof and wooden roof made with cement walls have shown a lower thoron concentration than others.

The final aspect has been studied broadly by categorising 106 houses into kaccha houses and pakka houses. Categorisation has been made on the point that those houses that have used mud for the roof/wall/floor are kaccha houses and the houses made with materials other than mud are pakka houses. Figure 17 illustrates that significant difference can be seen in the thoron concentration of kaccha houses and pakka houses. Kaccha houses have higher concentration of radon and thoron than pakka houses. Radium/thorium-rich soil is the main reason behind the higher concentration of radon/thoron in kaccha houses or mud houses (Kumar et al., 2014, Kumar and chauhan 2014).

**Influence of ventilation condition**

To study the effect of ventilation on the indoor concentrations of gases and progeny, dwellings were divided qualitatively into three categories: poor, average and good ventilation. The selection has been made on the basis of number of doors and windows

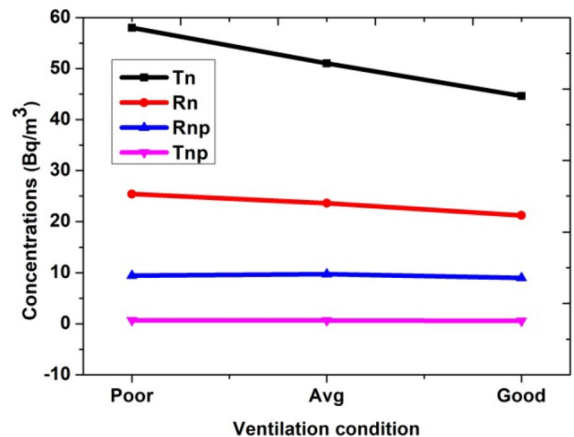


**Fig. 18** Radon/thoron and their progeny concentration under different ventilation conditions

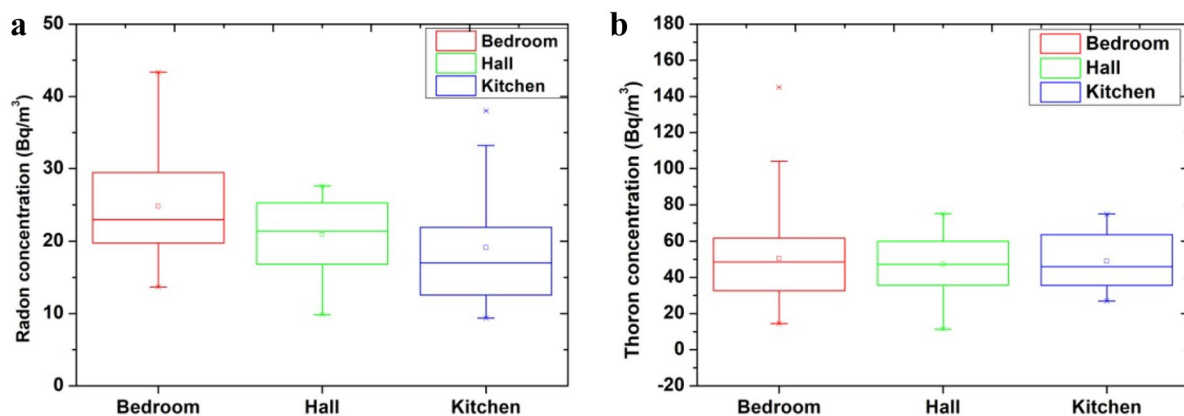


**Fig. 19** a Variation of radon and b thoron concentrations due to different rooms

in the room. Poorly ventilated rooms were those who have only one door, those with one door with one side window are considered average ventilated rooms and rooms with two doors and two side windows are considered well-ventilated rooms. With one door, air is stuck inside and cannot easily leave the room. It causes an increase in the air pollutants inside the room. Therefore, these rooms are termed as poorly ventilated rooms. In fully ventilated rooms (rooms having two doors and two windows), air circulates properly in the rooms and takes away all the pollutants outside and fresh air inside the rooms. Likewise, the rooms with one door and one window are considered average-ventilated rooms depending upon the positions of the window.

The study has revealed that the radon concentration has been reduced with increasing ventilation in

the room (Mehta et al., 2015) and same as with thoron concentration (Fig. 18). Higher radon concentrations in poorly ventilated rooms have been also reported in Mehra and Bala (2013) and Mehta et al. (2015), and a high thoron concentration in poorly ventilated rooms can be seen in Sathish et al. (2012). This is due to the difference in their half-lives. Thoron progeny has been found almost same for all ventilation conditions, which can also be seen in Ma et al. (1997).

#### Influence of room type

An attempt has also been made to study the variation of radon and thoron in different types of rooms, i.e. bedroom, hall (living room) and kitchen. It is shown that the radon concentration is found to be different in all room types because of different ventilation effects

**Table 5** Average indoor and outdoor gamma level, absorbed dose rate and annual effective dose equivalent in different houses of the Ludhiana district  
No. of measurements: 106 houses  
*Min* minimum, *Max* maximum, *Avg* average, *Med* median, *GM* geometric mean, *Stdev* standard deviation, *GSD* geometric standard deviation

	Gamma level (μSv/h)		Absorbed dose rate (nGy/h)		Annual effective dose equivalent (mSv/y)		Ratio (indoor/outdoor) annual effective dose equivalent
	Indoor	Outdoor	Indoor	Outdoor	Indoor	Outdoor	
<i>Min</i>	0.13	0.12	113.1	104.4	0.55	0.13	3.11
<i>Max</i>	0.25	0.23	217.5	200.1	1.07	0.25	6.46
<i>Avg</i>	0.19	0.17	166.94	144.78	0.82	0.18	4.66
<i>Med</i>	0.19	0.16	165.3	139.2	0.81	0.17	4.61
<i>GM</i>	0.19	0.16	165.5	143.4	0.81	0.18	4.61
<i>Stdev</i>	0.03	0.02	21.75	20.06	0.11	0.02	0.62
<i>GSD</i>	1.14	1.15					1.14

(Fig. 19a) and a higher concentration has been found in bedrooms relative to those in halls and kitchens. The probable reason is that bedrooms are less ventilated as compared to halls and kitchens. The thoron concentration has been found to be approximately the same in all due to the short half-life (Fig. 19b) as ventilation conditions do not affect the thoron concentration. Additionally, exhaust fans have been almost found in most of the kitchens, which can be the reason for the low radon concentration in kitchens.

### Comparison between indoor and outdoor terrestrial gamma radiation doses

The results of indoor and outdoor gamma radiation doses estimated during this study are summarised in Table 5. Indoor and outdoor absorbed dose rates varied from 113.1 to 217.5 nGy/h and 104.4 to 200.1 nGy/h, which are found to be higher than the world's average of 60 nGy/h ranging from 10 to 200 nGy/h (UNSCEAR, 2000b and Tuskin et al., 2009). The average annual effective dose for indoor and outdoor was obtained to be 0.82 mSv and 0.18 mSv, respectively, which are less than the ICRP (1990) recommended limit of 1 mSv. The indoor to outdoor dose ratios were ranging between 3.11 and 6.46.

### Conclusion

This study has been conducted in Ludhiana district of Punjab state, India. A total of 106 houses in 42 villages have been examined for assessment of radon/thoron and their progeny. This study was performed in order to explore the factors that are accountable for radon/thoron and their decay product concentration variations in the indoor environment. The indoor/outdoor terrestrial gamma radiation level has also been measured for these selected locations in this study. The indoor gamma radiation dose has been found to be 86% higher than the outdoor dose. The average indoor radon and thoron concentrations have been found to be ranging from  $9.4 \pm 1.6$  to  $43.4 \pm 4.7$  Bq/m<sup>3</sup> and  $11.4 \pm 3.1$  to  $145 \pm 11$  Bq/m<sup>3</sup>, respectively.

The average annual inhalation dose has been found to be 0.8 mSv/year, which is less than the world's

average inhalation dose, i.e. 1.2 mSv/year (UNSCEAR, 2000b). The contribution to the annual average effective dose due to radon progeny and thoron progeny was found to be 75% and 25%, respectively. In seasonal behaviour, higher radon and thoron concentrations have been found in the winter season whereas bedrooms of the study region showed higher concentrations than those measured in halls and kitchens. Both of these observations pertain to the role of ventilation in ascertaining the concentration levels.

**Author contribution** Supervision has been done by Dr. Amit Sarin. Dr. Navjeet Sharma and Anjali Kaushal have worked on the original draft, and formal analysis has been done by Manish Joshi. All authors read the manuscript and approved it for final submission.

**Funding** The Board of Research in Nuclear Sciences, Department of Atomic Energy, Mumbai, India, provided financial assistance under a major research project (Project No. 2013/36/54-BRNS) for this work. This work was also financially supported by DST Government of India under the FIST Scheme.

**Availability of data and materials** The datasets used and/or analysed during the current study are available from the corresponding author on reasonable request.

**Code availability** Not applicable.

### Declarations

**Conflict of interest** The authors declare no competing interests.

### References

- Bangotra, P., Mehra, R., Jakhu, R., et al. (2019). Quantification of an alpha flux based radiological dose from seasonal exposure to <sup>222</sup>Rn, <sup>220</sup>Rn and their different EEC species. *Science and Reports*, 9, 2515. <https://doi.org/10.1038/s41598-019-38871-6>
- Darby, S., Hill, D., Auvinen, A., Barros-Dios, J. M., Baysson, H., Bochicchio, F., Deo, H., Falk, R., Forastiere, F., Hakama, M., Heid, I., Kreienbrock, L., Kreuzer, M., Lagarde, F., Mäkeläinen, I., Muirhead, C., Oberaigner, W., Pershagen, G., Ruano-Ravina, A., ... Doll, R. (2005). Radon in homes and risk of lung cancer: Collaborative analysis of individual data from 13 European case-control studies. *BMJ*. <https://doi.org/10.1136/bmj.38308.477650.63>
- District survey report: district Ludhiana, Punjab. Retrieved September 27, 2017, from [http://www.ludhiana.nic.in/asp/dcoff/final\\_dsr.pdf](http://www.ludhiana.nic.in/asp/dcoff/final_dsr.pdf)
- Doi, M., Fujimoto, K., Kobayashi, S., & Yonohara, H. (1994). Spatial distribution of thoron and radon concentration in

- indoor air of a traditional wooden house. *Health Physics*, 66, 43–49.
- Edling, C., Wingreen, G., & Axelson, O. (1986). Quantification of the lung cancer risk from radon daughter exposure in dwellings – An epidemiological approach. *Environment International*, 12(1–4), 55–60.
- ICRP. (1990). *Recommendations of the International Commission on Radiological Protection*, 21, 1–3, publication 60.
- ICRP. (2011). International Commission on Radiological Protection: Radiological protection against radon exposure. Draft report for consultation.
- Jilek, K., Thomas, J., & Tomasek, L. (2010). First results of measurement of equilibrium factor F and unattached fractions fp of radon progeny in Czech dwellings. *Nukleonika*, 55(4), 439–444.
- Kumar, A., Chauhan, R. P., Joshi, M., Aggarwal, P. (2014). Implications of variability in indoor radon/thoron levels: A study of dwellings in Haryana, India. *Environmental Earth Sciences*. <https://doi.org/10.1007/s12665-014-3688-5>.
- Kumar, A., & Chauhan, R. P. (2014). Measurement of indoor radon-thoron concentration and radon soil gas in some North Indian dwellings. *Journal of Geochemical Exploration*, 143, 155–162.
- Kumar, M., Kaushal, A., Sarin, A., Kumar, R., Sharma, N. (2017). Radon/thoron and progeny levels in dwellings: Regional variations and effect of dwelling characteristics – A case study in Jalandhar district of Punjab, India. *Indoor Built Environment*, 27, 1420326X1668761. <https://doi.org/10.1177/1420326X16687614>
- Ludhiana district Punjab - Central ground water board. (2013). Retrieved September 27, 2017 from [http://www.cgwb.gov.in/district\\_profile/punjab/ludhiana.pdf](http://www.cgwb.gov.in/district_profile/punjab/ludhiana.pdf)
- Ma, J., Yonehara, H., Aoyama, T., Doi, M., Kobayashi, S., Sakanoue, M. (1997). Influence of air flow on the behaviour of thoron and its progeny in a traditional Japanese house. *Health Physics Society*, 72(1).
- Mehta, V., Singh, S. P., Chauhan, R. P., & Mudahar, G. S. (2015). Study of indoor radon, thoron, their progeny concentration and radon exhalation rate in the environs of Mohali, Punjab, Northern India. *Aerosol and Air Quality Research*, 15, 1380–1389.
- Mehra, R., Singh, S., & Singh, K. (2006). A study of uranium, radium, radon exhalation rate and indoor radon in the environs of some areas of Malwa region Punjab. *Indoor Built Environment*, 15(5), 499–505.
- Mehra, R., & Bala, P. (2013). Assessment of radiation hazards due to the concentration of natural radionuclides in the environment. *Environment and Earth Science*, 71, 901–909. <https://doi.org/10.1007/s12665-013-2493-x>
- Mishra, R., Tripathy, S. P., Khathing, D. T., & Dwivedi, K. K. (2004). An extensive indoor  $^{222}\text{Rn}/^{220}\text{Rn}$  monitoring in Shillong, India. *Radiation Protection Dosimetry*, 112(3), 429–433.
- Mishra, R., & Mayya, Y. S. (2008). Study of a deposition-based direct thoron progeny sensor (DTPS) technique for estimating equilibrium equivalent thoron concentration (EETC) in indoor environment. *Radiation Measurements*, 43, 1408–1416.
- Mishra, R., Mayya, Y. S., & Kushwaha, H. S. (2009). Measurement of  $^{220}\text{Rn}/^{222}\text{Rn}$  progeny deposition velocities on surfaces and their comparison with theoretical models. *Journal of Aerosol Science*, 40, 1–15.
- Mishra, R., Prajith, R., Sapra, B. K., & Mayya, Y. S. (2010). Response of direct thoron progeny sensors (DTPS) to various aerosol concentrations and ventilation rates. *Nuclear Instruments and Methods in Physics Research B*, 268, 671–675.
- Nazaroff, W. W., & Nero, A. V. (1988). *Radon and its decay products in indoor air*. JohnWiley & sons.
- Ningappa, C., Sannappa, J., Chandrashekar, M. S., & Paramesh, L. (2008). Concentrations of radon and its daughter products in and around Bangalore city. *Radiation Protection Dosimetry*, 130(4), 459–465.
- Omori, Y., Ganesh, P., Sorimachi, A., Sahoo, S. K., Ishikawa, T., Sagar, D. V., Ramola, R. C., & Tokonami, S. (2016). Long-term measurements of residential radon, thoron, and thoron progeny concentrations around the Chhatrapur placer deposit, a high background radiation area in Odisha, India. *Journal of Environmental Radioactivity*, 162–163, 371–378.
- Porstendorfer, J. (1984). Behaviour of radon products in the indoor air. *Radiation Protection Dosimetry*, 7, 107–113.
- Punjab Remote Sensing Centre, Ludhiana. Retrieved December 18, 2019, from <http://punenvvis.nic.in/WriteReadData/links/Picture10-706170806.jpg>
- Ramola, R. C., Negi, M. S., & Choubey, V. M. (2003). Measurements of equilibrium factor “F” between radon and its progeny and thoron and its progeny in the indoor atmosphere using nuclear track detectors. *Indoor and Built Environment*, 12, 351–355.
- Ramola, R. C., Prasad, M., Kandari, T., Pant, P., Bossew, P., Mishra, R., & Tokonami, S. (2016). Dose estimation derived from the exposure to radon, thoron and their progeny in the indoor environment. *Scientific Reports*, 6, 31061. <https://doi.org/10.1038/srep31061>
- Sannappa, J., Chandrasheker, M. S., Sathis, L. A., And, P. L., & Venkataramaiah, P. (2003). Study of background radiation dose in Mysore city, Karnataka state. *Radiation Measurements*, 37, 55.
- Sahoo, B. K., Sapra, B. K., Kanse, S. D., Gaware, J. J., & Mayya, Y. S. (2013). A new pin-hole discriminated  $^{222}\text{Rn}/^{220}\text{Rn}$  passive measurement device with single entry face. *Radiation Measurements*, 58, 52–60.
- Sathish, L. A., And, N. K., & Ramachandran, T. V. (2012). Indoor  $^{222}\text{Rn}$  and  $^{220}\text{Rn}$  concentrations and doses in Bangalore. *Radiation Protection and Environment*, 151(2), 344–353.
- Sesana, L., Caprioli, E., & Marcazzan, G. M. (2003). Long period study of outdoor radon concentration in Milan and correlation between its temporal variations and dispersion properties of atmosphere. *Journal of Environmental Radioactivity*, 65, 147–160.
- Sevc, J., Kunz, E., & Placek, V. (1976). Lung cancer in uranium miners and long-term exposure to radon daughter products. *Health Physics*, 30(6), 433–437.
- Singh, P., Saini, K., Mishra, R., Sahoo, B. K., & Bajwa, B. S. (2016). Attached, unattached fraction of progeny concentrations and equilibrium factor for dose assessments from  $^{222}\text{Rn}$  and  $^{220}\text{Rn}$ . *Radiation and Environmental Biophysics*. <https://doi.org/10.1007/s00411-016-0656-3>
- Smetsers, R. C. G. M., & Tomas, J. M. (2019). A practical approach to limit the radiation dose from building materials applied in dwellings, in compliance with the Euratom Basic Safety Standards. *Journal of Environmental Radioactivity*, 196, 40–49.
- Stojanovska, Z., Januseski, J., Bossew, P., Zunic, Z. S., Tollefsen, T., & Ristova, M. (2011). Seasonal indoor radon concentration in FYR of Macedonia. *Radiation Measurements*, 46, 602–610.

- Stojanovska, Z., Bossew, P., Tokonami, S., Zunic, Z. S., Bochicchio, F., Boev, B., Ristova, M., & Januseski, J. (2013). National survey of indoor thoron concentration in FYR of Macedonia (continental Europe – Balkan region). *Radiation Measurements*, *49*, 57–66.
- Taskin, H., Karavus, M., Ay, P., Topuzoglu, A., Hidiroglu, S., & Karahan, G. (2009). Radionuclide concentrations in soil and lifetime cancer risk due to gamma radioactivity in Kırklareli. *Journal of Environmental Radioactivity*, *100*, 49–53.
- UNSCEAR. (1988). United Nations Scientific Committee on the Effects of Atomic Radiation. Sources effects and risks of ionizing radiation, Report to the General Assembly, United Nations, New York.
- UNSCEAR. (1993). United Nations Scientific Committee on the Effects of Atomic Radiation. Effects and risks of ionizing radiation. Annex – B: Exposure from natural sources of radiation, United Nations, New York.
- UNSCEAR. (2000a). United Nations Scientific Committee on the Effects of Atomic Radiation. Annex B: Exposures from natural radiation sources. United Nations, 104.
- UNSCEAR. (2000b). United Nations Scientific Committee on the Effects of Atomic Radiation, Sources and effects of ionizing radiation, United Nations, New York.
- UNSCEAR. (2008). United Nations Scientific Committee on the Effects of Atomic Radiation. Report to the General Assembly, United Nations, New York.
- Virk, H. S., Sharma, N. (2000). Indoor radon levels and inhalation doses to population in Punjab. *Current Science*, *78*(12), 1418–1420.
- Yu, K. N., & Nikezic, D. (1996). Long-term determination of airborne radon progeny concentrations using LR 115 solid-state nuclear track detectors. *Radiation Measurements*, *46*, 1799–1802.
- Zhuo, W., Iida, T., & Yang, X. (2000). Environmental radon and thoron progeny concentrations in Fujian of China. *Radiation Protection Dosimetry*, *87*, 137–140.

**Publisher's Note** Springer Nature remains neutral with regard to jurisdictional claims in published maps and institutional affiliations.